LUMINESCENCE CHARACTERIZATION OF TB^{3+} DOPED BAALSI$_5$O$_2$N$_7$ PHOSPHOR

S.A.Fartode[1] Anoop Fartode[2], S.J.Dhoble[3]
[1]Department of Physics, Dr. Babasaheb Ambedkar College of Engineering and Research, Nagpur, India
[2]Department of Chemistry, K.D.K. College of Engineering, Nagpur, India
[3]Department of Physics, RTM Nagpur University, Nagpur, India

Abstract

The nitride phosphors are useful for lighting application. Recently nitride phosphors has attracted interest owing to their hardness, fracture strength , toughness, wear resistance, outstanding thermal and chemical stability, thermal resistivity, wide band gap and luminescent properties.

In this communication, synthesis and luminescent properties of Tb^{3+} activated BaAlSi$_5$O$_2$N$_7$ oxinitride phosphor are reported. The material was synthesized through modified two step high temperature solid state diffusion technique. The prepared sample was confirmed by XRD technique. The Tb^{3+} activated BaAlSi$_5$O$_2$N$_7$ material shows efficient blue green emission under 270 nm excitation. The emission spectrum composed of two groups of lines in the wavelength range of 400-650 nm. One group in the range 490-650 nm corresponding to $^5D_4$ → ^7F_J (J = 6,5,4,3) transitions of Tb^{3+} and other in range 400- 470 nm originating from the $^5D_3$→ ^7F_J (J = 6,5,4,3,2,1,0) transitions of Tb^{3+}. It is well known that Tb^{3+} concentration affects the relative intensities of $^5D_4$ and $^5D_3$ emissions of Tb^{3+} activated samples. The variation of Tb^{3+} concentration with intensity was also studied.

Keywords: BaAlSi$_5$O$_2$N$_7$; mechano luminescence;. phosphor; photoluminescence; solid state diffusion method;

I. Introduction:

To meet the ever increasing demand of white LED lighting, Eu^{2+}, Ce^{3+} and Tb^{3+} activated aluminosilicon nitride-based luminescent materials have been rapidly developed [1]-[8]. Siliconoxynitride/nitride-based compounds have unique structural features due to the presence of nitrogen in the lattices [9]–[13]. Hence, appropriate difference in the luminescence properties is expected for Eu^{2+} and Tb^{3+} activator ions. Due to high degree of covalent bonding and large crystal field splitting of 5d excited levels the excitation and emission bands of these ions can be shifted to lower energies [14]. Eu^{3+}, Tb^{3+}, Dy^{3+} and Tm^{3+} ions show unique optical behavior when doped into host material. The electronic transitions occurring within the partially filled 4f energy shell of the lanthanide series contributes to the luminescence of these ions [15]. Particularly for efficient blue–green emissions, Tb^{3+} ions are used as activators. This begins from the transitions of $^5D_3$ and $^5D_4$ excited states to ^7F_J (J=0, 1… 6) ground states of Tb^{3+} ions. For UV radiation excitation, Tb^{3+} ions are raised to higher $4f^75d^1$ level from $4f^8$ and afterward raised to $^5D_3$ or $^5D_4$ excited states [16] Tb^{3+} activated phosphors have been widely used in various applications such as X-ray intensifying screens, three-band fluorescent lamps and projection television tubes [17]. In general all thermoluminescent materials also show ML during their deformation [18]. In present communication; photoluminescence, mechanoluminescence and thermoluminescence properties of Eu^{2+}, Ce^{3+} and Tb^{3+} activated BaAlSi$_5$O$_2$N$_7$oxinitride phosphor are discussed.

II. EXPERIMENTAL TECHNIQUE

Polycrystalline BaAlSi$_5$O$_2$N$_7$:Tb^{3+} samples were synthesized by high temperature modified two step solid-state diffusion techniques. The starting

materials were high purity $BaCO_3$ (Merck, >99.0%), α-Si_3N_4 powder, Al_2O_3, $Al(NO_3)_3$, Tb_2O_3 of AR grade. The appropriate amounts of starting materials were weighed out separately on an analytical balance and subsequently mixed and ground together in an agate mortar. The powder mixtures were then transferred into crucibles and were fired in a horizontal tube furnace (muffle furnace) at 800 ℃ for 24 hours. The samples were gradually cooled down to room temperature in furnace. $BaAlSi_5O_2N_7$:Tb^{3+} sample was again fired in a furnace at 1200 ℃ for four hours and all the samples were pulverized for further measurements.

The XRD measurements of the prepared phosphors were performed at room temperature in air. The composition and phase purity of the products were measured by powder X-ray diffraction (XRD) analysis with an X'Pert PRO diffractometer with Cu-Kα radiation (λ= 1.54060 Å) operated at 45 kV and 40 mA. The XRD data were collected in a 2θ range from 10° to 100°. The photoluminescence (PL) emission spectra of the samples were recorded using spectrofluorophotometer (shimadzu RF-5301). The same amount of sample was used in each case. The emission and excitation spectra were recorded using spectral slit width of 1.5nm. The mechanoluminescence (ML) in γ-irradiated Tb doped $BaAlSi_5O_2N_7$ is done by RCA 931A photomultiplier tube connected to a storage oscilloscope (Scintific HM-205). For determining the peak intensity, peak position, rise and decay time of ML, trace on the oscilloscope screen was recorded on tracing paper.
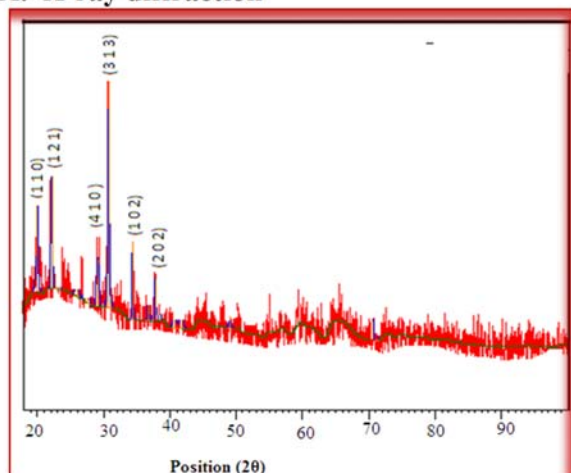
III. RESULTS AND DISCUSSION
A. X-ray diffraction

Fig.1 XRD pattern of $BaAlSi_5O_2N_7$

Fig.1 shows the XRD pattern of $BaAlSi_5O_2N_7$ sample. The XRD pattern of the prepared sample matched with the XRD pattern reported by Duan *et al.* [19]. The Miller indices of major peaks of XRD are also shown in Fig.

B. FTIR of $BaAlSi_5O_2N_7$:Tb^{3+} In FTIR, electromagnetic radiations are absorbed by material in the infrared region of the spectrum which changes the vibration energy of molecule. Since all molecules usually possess vibrations in form of stretching, bending etc. the absorbed energy will be utilized in changing the energy levels associated with these. FTIR is an important tool for identification and structural analysis of organic compounds, natural products, polymers etc.

When an infrared light interacts with the matter, chemical bonds will stretch, contract and bend. As a result, a chemical functional group tends to absorb infrared radiation in a specific wave number range regardless of the structure of the rest of the molecule [20]. The IR spectra of the sample in the wave number range from 4000 to 400 cm^{-1} as a function of percentage transmittance is reported in Fig.2
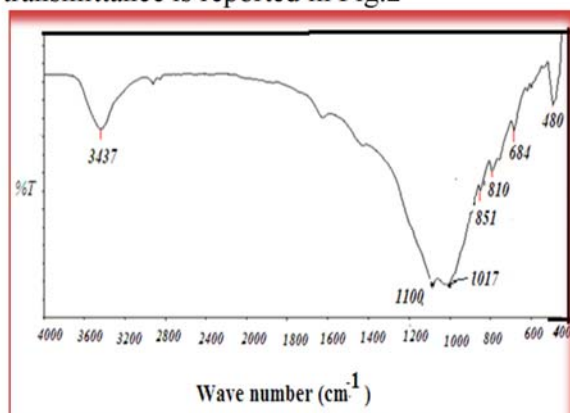

Fig.2 FTIR spectra of $BaAlSi_5O_2N_7$:Tb^{3+}

The IR spectrum of the sample has absorption band at 3437 cm^{-1} due to weak stretching of N-H bond. The absorption band at 1100 cm^{-1} and 810 cm^{-1} could be allocated to asymmetric stretching of Si-O-Si [21]. The asymmetric stretching of M-ONO is found at 1017 cm^{-1}. The weak band at 851 cm^{-1} occurs due to stretching of N-O bond [20]. The band observed at 684 cm^{-1}, 599 cm^{-1} and 480 cm^{-1} are assigned to bending of M=O, M-NO_2, and Y-(0) N respectively [20],[21].

C. Photoluminescence of $BaAlSi_5O_2N_7$:Tb^{3+}

Under 270 nm excitation, $BaAlSi_5O_2N_7$:Tb^{3+} emits bright blue green light (Fig. 3). The emission spectrum (Fig. 4) of Tb^{3+} in

$BaAlSi_5O_2N_7$ is composed of two groups of lines in the wavelength range of 400-650nm: one group in the range 490-650nm corresponding to $^5D_4 \rightarrow ^7F_J$ (J = 6,5,4,3) transitions of Tb^{3+} and other in range 400- 470nm originating from the $^5D_3 \rightarrow ^7F_J$ (J = 6,5,4,3,2,1,0) transitions of Tb^{3+}. The dominant one is $^5D_4 \rightarrow ^7F_5$ at about 544 nm. The emission peak due to $^5D_4 \rightarrow ^7F_5$ transition split into two peaks; one at 544nm and other at 552 nm due to crystal field effect [22]. It is well known that Tb^{3+} concentration affects the relative intensities of $^5D_4$ and $^5D_3$ emissions of Tb^{3+} activated samples.

As the concentration of Tb^{3+} increases, the emission intensity increases from 0.05 mole % to 1 mole % and then decreases for 2 mole %. As the concentration of Tb^{3+} ion exceeds 1 mole %, interaction between Tb^{3+} ions itself takes place rather than having interaction between Tb^{3+} and host. This happens due to concentration quenching [23].
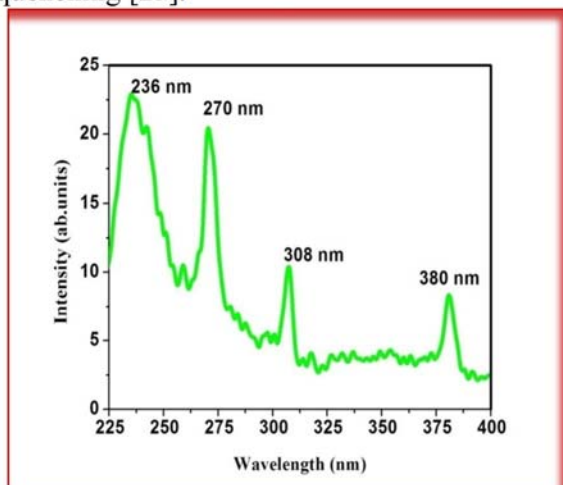

Fig. 3 Photoluminescence excitation spectrum of $BaAlSi_5O_2N_7:Tb^{3+}$

Normally a blue emission originating from $^5D_3$ level is mainly observed at a low Tb^{3+} concentration [22]. The non radiative decay from $^5D_3$ state to $^5D_4$ state via cross relaxation ($^5D_3 \rightarrow ^5D_4 \geq ^7F_6 \rightarrow ^7F_0$ and $^5D_3 \rightarrow ^7F_0 \geq ^7F_6 \rightarrow ^5D_4$) is probable if the Tb^{3+} ions are present at short distances and this results in a change from blue to green emission [20]. For a system where Tb^{3+} ions are distributed homogeneously, above change is observed when the Tb^{3+} concentration is increased above the critical Tb^{3+} concentration for cross relaxation [23]. In excitation spectrum (Fig.3) some peaks are observed in the wavelength range of 230-400 nm which can be ascribed to the transitions between the energy levels within $4f^8$ configuration

i.e. $^7F_6 \rightarrow ^5D_3$ ($\approx$ 380nm) [22]. The peak at 270nm in excitation spectra of $BaAlSi_5O_2N_7:Tb^{3+}$ may be attributed to $BaAlSi_5O_2N_7$ host absorption and terbium–oxygen charge-transfer respectively [24].

The ground states for Tb^{3+} ions are ^7F_J with $4f^8$ electron configuration. The transformation of one electron to 5d shell produced two $4f^75d^1$ excited state one the high spin state with ^9D_J configuration and another the low spin state with ^7D_J configuration. But it was noticed that ^7D_J state is higher in energy than ^9D_J state. The Hund's rule suggested that the transitions between ^7F_J and ^7D_J are spin allowed while the transition between ^7F_J and ^9D_J are spin-forbidden.
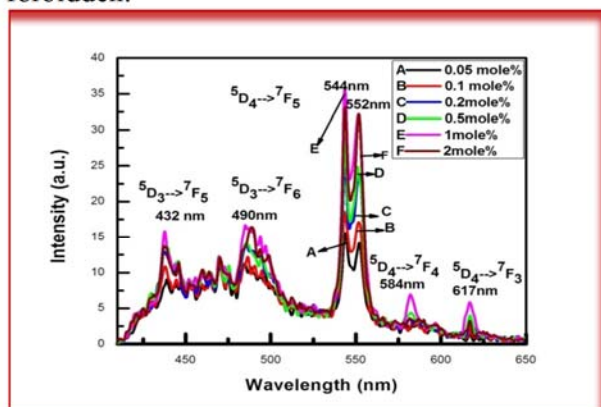

Fig. 4 Photoluminescence emission spectra of $BaAlSi_5O_2N_7:Tb^{3+}$

Therefore a specific host with Tb^{3+} ion exhibits two groups of f-d transition: at high energy the spin-allowed f-d transitions are strong and the spin-forbidden f-d transitions are weak at low energy [25]. The energy diagram of the luminescence of the $BaAlSi_5O_2N_7:Tb^{3+}$ phosphor is shown in Fig.5.
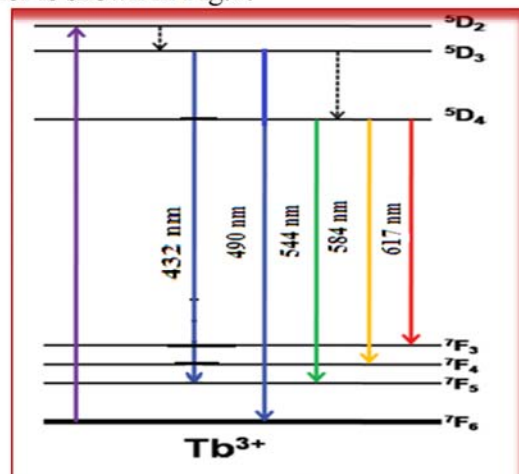

Fig. 5 schematic diagram showing the transition of Tb^{3+} ions

D. Mechanoluminescene study of BaAlSi₅O₂N₇:Tb³⁺

ML glow curve for different impurity concentration, impact velocity, ML spectra, height and mass can be viewed in Figures 6, 7, 8, 9, 10 and 11 respectively. The phosphor has a single glow curve with a single mechanoluminescence peak.

Fig. 6 shows the time dependence of ML intensity of BaAlSi₅O₂N₇: Tb³⁺sample for the different concentrations of impurities. It is clear that ML intensity increases with increasing concentration of impurities. Fig. 6 reflects that ML intensity was maximum for 1 mole % and for higher values of impurity concentration ML intensity decreases suggesting that the concentration quenching of luminescence centre may take place. ML intensity initially increased with time, attained an optimum value for a particular time and then decreased and finally disappeared for all the samples. However there is no considerable change in t_m (*i.e.* the time corresponding to ML peak).
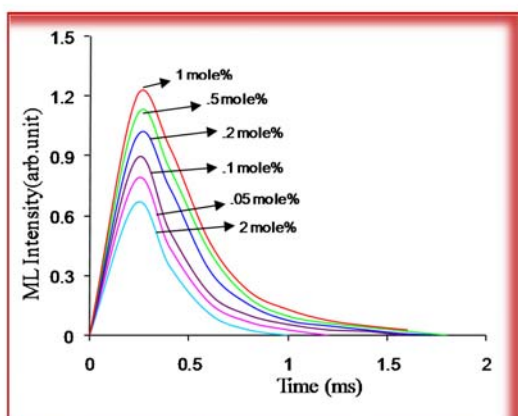

Fig. 6 Time dependence of ML intensity of BaAlSi₅O₂N₇:Tb³⁺ samples for the different concentrations of impurities

Fig. 7 shows the ML glow curves of γ - irradiated rare earth Tb activated BaAlSi₅O₂N₇:Tb samples for different impact velocities of the piston. In all phosphors, maximum intensity is shown at 1 mole% of Tb activated barium based phosphor. It is seen that the ML intensity increases with increasing impact velocity. However the time corresponding to ML peak (t_m) shifts towards shorter time values with increasing impact velocity. Fig. 8 shows variation of total ML intensity with impact velocity. The total ML intensity of γ-irradiated Tb doped BaAlSi₅O₂N₇ increases linearly with increasing impact velocity of the piston of different mass and

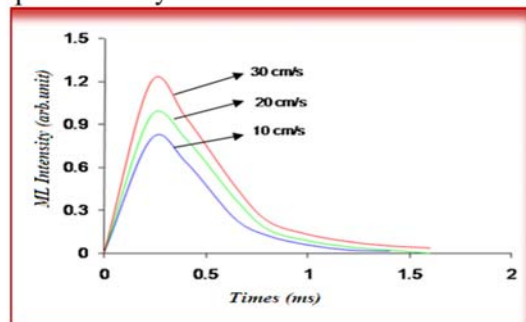attains a maximum value for higher value of impact velocity.

Fig. 7 ML glow curves of γ -irradiated BaAlSi₅O₂N₇: Tb³⁺ samples for different impact velocities of the Piston
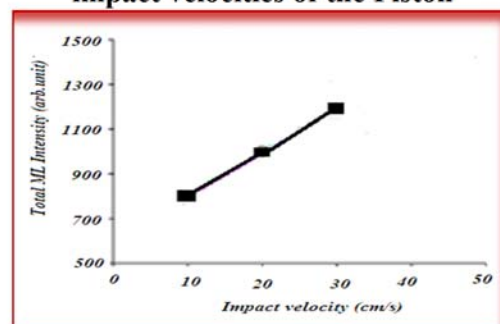
Fig. 8 Variation of total ML intensity with impact velocityfor BaAlSi₅O₂N₇: Tb³⁺
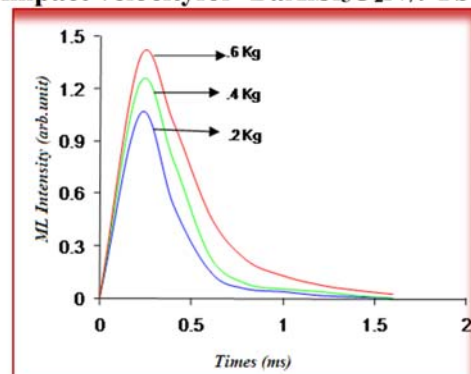
Fig. 9 ML intensity versus time curves of BaAlSi₅O₂N₇: Tb³⁺ for different mass of the piston
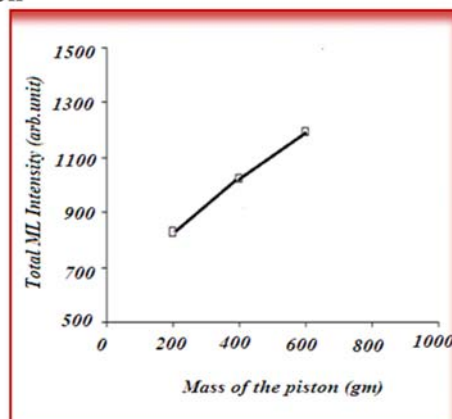
Fig. 10 Variation of total ML intensity with mass of the piston for BaAlSi₅O₂N₇: Tb³⁺
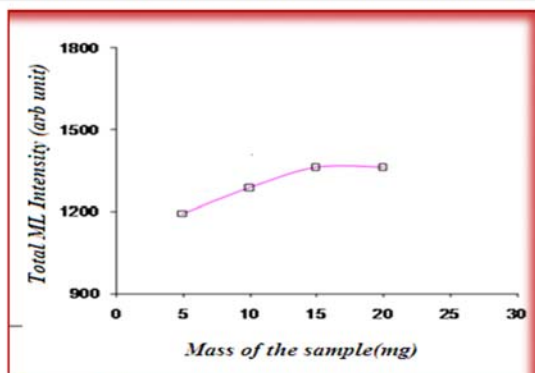
Fig. 11 ML glow curves for different mass of BaAlSi$_5$O$_2$N$_7$: Tb^{3+}

ML intensity increases almost linearly with increasing the mass (0.2 to 0.6 kg) of the piston. For recording ML, the samples were irradiated with gamma-ray dose of 0.037 kGy at the dose rate of 0.32 kGy/hr. When the mass of the piston increases, the number of newly created surface in the sample increases and thereby the ML intensity.

Fig. 9 and Fig. 10 shows the ML intensity versus time curves of samples for different mass of the piston dropped on BaAlSi$_5$O$_2$N$_7$:Tb^{3+}. The ML intensity initially increases with time, attains maximum value and then decreases for different mass of piston.

Fig. 11 shows the variation of total ML intensity with mass of the sample. As mass of the sample increases ML intensity increases up to 15 mg of sample and then remains constant.

It is suggested that barium based phosphor is strongly related to the movement of dislocations and the recombination of activated electrons and holes.

The movements of dislocations excite carriers from the filled traps and the subsequent recombination of the electrons and holes occur in luminescence centers (Tb^{3+}).

The appearance of ML in barium based phosphor indicates that ML in this material may not be due to the mechanical or electrostatic interaction between the bending segments of dislocations and filled hole traps because there is no possibility of dislocations in nano particles. Since only one peak is observed in ML intensity versus time curve it seems that capturing of carriers by the shallow traps is not taking place in this phosphor.

IV. CONCLUSIONS

The synthesis of BaAlSi$_5$O$_2$N$_7$ phosphor doped with Tb^{3+}was carried out using the high temperature modified three step solid state diffusion method. The series of Tb^{3+} in the BaAlSi$_5$O$_2$N$_7$ phosphors with various concentrations of dopant (0.05 mole % to 1.5 mole %) was prepared and the effect of doping concentration on the emission intensity for the phosphors was investigated. From the excitation and emission spectra, the BaAlSi$_5$O$_2$N$_7$:Tb^{3+} phosphors can be effectively excited by UV light (270 nm). It exhibited a satisfactory green emission (544nm) widely applied as UV LED chip.

ML intensity increases with increasing concentration of impurity. When a load is applied on the sample, initially the ML intensity increases with time, attains a peak value I_m at a particular time t_m and later on it decreases with time. Intensity also increases with height through which the load is dropped on the sample. When the sample is deformed elastically by dropping a load of small mass from a low height then initially the ML intensity increases with time, attains a peak value and later on it decreases with time. Intensity increases with height through which the load is dropped on the sample. ML intensity increases linearly with the density of filled hole traps. The trapping and de-trapping of charge carriers in the material can be studied using ML. This fundamental work might be important in developing new luminescent devices applicable for ML sensors and dosimeter.

REFERENCES

[1] R.J. Xie and N. Hirosaki, Silicon based oxinitride and nitride phosphor for white LED's:A Review Sci. Tech. Adv. Mater., vol. 8 pp. 588- 600, October 2007.

[2] Y.Q. Li, J.E.J. van Steen, J.W.H. van Krevel, G. Botty, A.C.A. Delsing, F.J. DiSalvo, G. de With and H.T. Hintzen, Luminescence properties of red emitting red emitting M2Si5O2N7:Eu2+(Ca,Sr,Ba) J. Alloys and Compd.,vol.417, pp.273- 279 , 2006

[3] Y.Q. Li, G. de With and H.T. Hintzen, The effect of replacement of Sr by Ca on the structural and luminescence properties of the red-emitting Sr$_2$Si$_5$N$_8$:Eu^{2+}LED conversion phosphor J. Solid State Chem., Vol.181,pp.515-524, March 2008.

[4] Y.Q. Li, N. Hirosaki, R.J. Xie, T. Takeda and M. Mitomo, Yellow-Orange-Emitting CaAlSiN $_3$:Ce $^{3+}$ Phosphor: Structure, Photoluminescence, and Application in White

LEDs Chem. Mater., vol.20, pp. 6704-6714,October 2008.

[5] K. Uheda, N. Hirosaki, Y. Yamamoto, A. Naito, T. Nakajima and H.Yamamoto Luminescence Properties of a Red Phosphor, $CaAlSiN_3 : Eu^{2+}$, for White Light-Emitting Diodes Electrochem. Solid-State Lett.,vol- 9,pp. H22-H25, February 2006.

[6] K. Uheda, N. Hirosaki and H. Yamamoto, Host lattice materials in the system Ca_3N_2–AlN–Si_3N_4 for white light emitting diode Phys. Stat. Sol. A, vol. 203, pp.2712-2717, September 2006.

[7] H. Watanabe, H. Yamane and N. Kijima, Crystal Structure and Luminescence of Sr0.99Eu0.01AlSiN3. J. Solid State. Chem., vol. 181 pp.1848-1852, April 2008

[8] H. Watanabe and N. Kijima, Crystal structure and luminescence properties of SrxCa1−xAlSiN3: Eu2+ mixed nitride phosphors J. Alloys and Compd., vol. 475 pp.434-439 May 2009.

[9] D.H. Gregory, Structural families in nitride chemistry J. Chem. Soc., Dalton Trans.issue 3pp.259-270 1999.

[10] W. Schnick and H. Huppertz, Nitridosilicates-A Significant Extension of Silicate Chemistry J. Chem. Eur.,vol 3pp.679-683, May 1997.

[11] R. Marchand, F. Tessier, A. Sauze, Diot and N. Le, Typical features of nitrogen in nitride-type compounds Intern J. Inorg. Mater., vol.3,pp.1143-1146, December2001

[12] W. Schnick Review Superelectrophiles Chem. Intern. Ed. Engl.,vol. 32,pp.805-827 June 1993.

[13] R. Niewa and F.J. DiSalvo, Recent Developments in Nitride Chemistry Chem. Mater., vol.10,pp.2733-2752, October 1998.

[14] J.W.H. van Krevel, H.T Hintzen, R. Metselaar and A. Meijerink, Long wavelength Ce^{3+} emission in Y–Si–O–N materials J. Alloys and Compd vol. 268 pp.272-277, March 199

[15] S.C. Gedam, S.J. Dhoble and S.V. Moharil, $5d \rightarrow 4f$ transition in halosulphate phosphors J. Lumin., vol.126,pp. 121-126 ,June 2007

[16] J.Y. Park, H.C Jung, G.S.R. Raju, B.K. Moon J.H. Jeong and J.H. Kim, J.Lumin., Vol. 130(2010)478.

[17] S.P. Khatkar, S.D. Han, V.B Taxak, G Sharma and D. Kumar, The influence of sintering temperature on particle size/shape and photoluminescence characteristics of CaIn2O4: xTb synthesized by combustion process. Opt. Mater.vol. 29pp.1362-1366, July 2007.

[18] N. Brahme, D.P Bisen, R.S Kher and M.S.K Khokhar, Mechanoluminescence and thermoluminesence in γ-irradiated rare earth doped CaF2 crystals Physics Procedia Vol. 2, pp.431-440, August 2009.

[19] C.J. Duan, W.M.Otten, A.C.A.Delsing and H.T.Hintzen, Photoluminescence properties of Eu^{2+}-activated sialon S-phase BaAlSi5O2N7 J. Alloys and Compd.,vol. 461 pp.454-458,August 2008.

[20] Dr.J.Cooke,Department of chemistry, (2005). University of Alberta

[21] D. Geng, H. Lian, M. Shang, Zhang Y and J Lin., Oxonitridosilicate Y10(Si6O22N2)O2:Ce3+ ,Mn2+ phosphors: a facile synthesis via the soft-chemical ammonolysis process, luminescence, and energy-transfer properties. J.inorg.Chem., vol. 53 pp. 2230-2239, February 2014

[22] P. Li, L. Pang, Z. Wang, Z. Yang, Q. Guo and X. Li, Luminescent characteristics of $LiBaBO_3:Tb^{3+}$ green phosphor for white LEDJ. Alloys and Compds.,vol. 478, pp. 813-815 June 2009.

[23] X Zhang, X. Qiao and H.J. Seo, Red Emission $LaMoBO_6 : Eu^{3+}$ Phosphor for Near-UV White Light-Emitting Diodes J.Electrochem. Soc., vol.157pp J267- J269May 2010.

[24] B. Chen, J. Yu and X. Liang Langmuir, vol.27,pp. 11654-11659, August 2011.

[25] Z.Zhang , M. K. Otmar, A. K. Delsing, vander Erik, H.L Notten Peter,P. Dorenbos, J. Zhao and H. T Hintzen Photoluminescence properties and energy level locations of RE3+ (RE= Pr, Sm, Tb, Tb/Ce) in CaAlSiN3 phosphors. J.Mater.Chem., vol.22pp. 9813-9820 January 2012.